Chemical Engineering Journal 98 (2004) 213–218

Chemical Engineering Journal

www.elsevier.com/locate/cej

Liquid phase mixing in 2-phase liquid–solid inverse fluidized bed

T. Renganathan, K. Krishnaiah*

Department of Chemical Engineering, Indian Institute of Technology Madras, Chennai 600036, India

Received 25 January 2003; accepted 1 August 2003

Abstract

Liquid phase residence time distribution studies are reported in 2-phase inverse fluidized bed for the first time in the literature. Using a pulse tracer technique and deconvolution method of analysis, RTD of the system, residence time, Peclet number and dispersion coefficient are determined. The liquid phase axial dispersion coefficient increases with increase in liquid velocity and Archimedes number and is independent of static bed height. An empirical correlation has been proposed for liquid phase axial dispersion coefficient in 2-phase IFB.

Keywords: Liquid–solid fluidization; Inverse fluidized bed; Residence time distribution; Axial dispersion; Deconvolution method

1. Introduction

Inverse fluidization is an operation in which solid particles having density lower than that of the liquid are kept under suspension supported by the downward flow of continuous liquid phase. In 3-phase inverse fluidized bed (IFB), gas is introduced countercurrently to the liquid as dispersed phase. Fan [1] classified all the gas–liquid–solid fluidization systems and identified IFB operation as mode E-II-a-1. Inverse fluidization has several advantages such as high mass transfer rates, minimum carry over of coated microorganisms due to less solids attrition, efficient control of biofilm thickness and ease of refluidization in case of power failure. These significant advantages found many applications of inverse fluidized beds in biochemical processes like ferrous iron oxidation [2] and aerobic and anaerobic biological wastewater treatment like treatment of wine distillery wastewater [3].

For successful analysis, design and operation of IFB reactor, information on hydrodynamics, heat and mass transfer characteristics, kinetics and contacting pattern is essential. Information on contacting pattern of the liquid phase is required for the efficient design and operation of IFB reactor. Liquid phase mixing greatly influences the heat and mass transfer rates and reactant conversion in any reactor. For example, an increase in axial mixing reduces the driving force of the transport processes and reduces the level of conversion. Hence, a quantitative estimation of mixing of phases is a key factor.

In spite of potential applications of 2-phase IFB in biochemical processes [2] and wastewater treatment [3], it is surprising to note that, not even a single study on axial mixing of liquid phase in 2-phase IFB is available in the literature even though contacting pattern of fluid phase is very important. Hence, in this paper an attempt is made to characterize the liquid phase mixing through RTD studies by varying parameters such as particle size and density, static bed height and liquid velocity.

2. Experimental details

A schematic diagram of the experimental setup of an inverse fluidized bed is shown in Fig. 1. The column was made of acrylic with an i.d. of 89 mm and an o.d. of 97 mm using multiple sections. The total height of the column was 2.8 m and that of test section was 1.86 m. A packed bed of berl saddles was used at the top of the column to provide uniform distribution of liquid.

Water was pumped from a storage tank through calibrated rotameters and admitted at the top of the column through distributor. Different rotameters were used to cover wide range of liquid flow. The water exited from the bottom of the column and recirculated back to the storage tank through an overflow weir. The overflow weir helps to maintain a constant water level in the column.

A 1 in. hole was provided in the middle of the test section for loading and unloading of particles. A wire mesh at the

* Corresponding author. Tel.: +91-44-2257-8211; fax: +91-44-2257-0509.
E-mail address: krishnak@iitm.ac.in (K. Krishnaiah).

1385-8947/$ – see front matter
doi:10.1016/j.cej.2003.08.001

Nomenclature

Ar	Archimedes number ($Ar = d_p^3(\rho_l - \rho_p)\rho_l g/\mu_l^2$)
d_p	diameter of particle (m)
D_l	liquid phase axial dispersion coefficient (m^2/s)
$E(t)$	exit age distribution (s^{-1})
$E(\theta)$	dimensionless exit age distribution
$E_{in}(t)$	exit age distribution measured at 1st measuring point (s^{-1})
$E_{out}(t)$	exit age distribution measured at 2nd measuring point (s^{-1})
$E_{out,prd}(t)$	exit age distribution predicted at 2nd measuring point using deconvolution procedure (s^{-1})
$f(\tau,Pe)$	axial dispersion model impulse response function
g	acceleration due to gravity (m/s^2)
H_0	static bed height
J	objective function (s^{-2})
Pe	liquid phase Peclet number ($Pe = u_l \Delta z/D_l\varepsilon$)
Re	liquid Reynolds number ($Re = u_l d_p \rho_l/\mu_l$)
Re_{mf}	liquid Reynolds number at minimum fluidization for 2-phase IFB ($Re_{mf} = u_{mf} d_p \rho_l/\mu_l$)
t	time (s)
u_l	liquid velocity (superficial) (m/s)
u_{mf}	liquid velocity at minimum fluidization for 2-phase IFB (m/s)
Δz	distance between measuring points (m)

Greek letters

ε	average void fraction of bed
μ_l	liquid viscosity (kg/m s)
θ	dimensionless residence time of liquid
ρ_l	liquid density (kg/m^3)
ρ_p	particle density (kg/m^3)
τ	mean residence time of liquid from RTD studies (s)
τ_{hyd}	mean residence time of liquid from hydrodynamic studies (s)

top of the column and another above the bottom distributor help to retain the particles within the test section. During RTD experiments, the outlet water with tracer coming out of the overflow weir was diverted to a collection tank. A septum was provided at the top of the column before the liquid distributor for injecting the tracer.

Provisions were made for online measurement of tracer by the conductivity method. To measure the conductivity, SS 314 electrodes (10 mm × 10 mm cross-section and 20 mm length) were fixed with the inside surface flush with the wall of the column. This arrangement would not hinder the free movement of fluidized particles in the column. A pair of electrodes was placed diametrically opposite with the longer side perpendicular to the axis of the column. Eighteen sets of such electrodes were placed at an equal distance of 10 cm along the length of the column. To record the online conductivity measurements, the electronic circuit consisting of a switching circuit, a conductivity meter and an A/D card (16 bit, 16 channel, loaded in a computer) was fabricated. The switching circuit used to switch between the 18 electrodes can be operated automatically using a software trigger from the computer or manually.

Table 1
Range of variables

Variable	Range
Particle diameter (mm) (density, kg/m^3)	0.18 (693), 2.34[a] (897), 6.1 (917), 12.2 (835), 12.6 (250)
Liquid velocity (cm/s)	0.02–10
Static bed height (cm)	15, 30, 45

[a] Equivalent diameter of cylindrical particle.

Pulse input method was used in the present work to measure the RTD of liquid phase. Since injecting a perfect pulse input of tracer was difficult, the liquid phase mixing studies were analyzed using an imperfect pulse method by recording the concentration of tracer at two different locations inside the bed. In a typical RTD experiment, for a chosen particle, bed height and liquid flow rate, the system was allowed to reach steady state. A pulse of 3 ml of 5N NaCl solution was injected using a syringe through the septum at the top of the column. The time taken for the tracer injection in all the experiments was less than one-third of a second.

The concentration in terms of voltage was simultaneously measured at two electrodes well within the bed at a frequency of 25 Hz using the online data acquisition system. The voltage data was converted to salt concentration using calibration equation based on separate experiments. The experiment was repeated for different liquid flow rates, static bed heights and particle characteristics. The range of variables used for RTD studies are presented in Table 1. Most of the experiments were repeated at least for 5 times and some experiments for 10 times. This was necessary since the mean residence time of liquid for some experimental conditions falls within a few seconds. The concentrations are obtained by smoothening the raw data using piecewise splines [4].

3. Deconvolution procedure

Since the imperfect pulse method is used, the deconvolution procedure proposed by Michelsen [5] is adopted to obtain the RTD and the Peclet number of the system represented by the fluidized bed between the two measuring points.

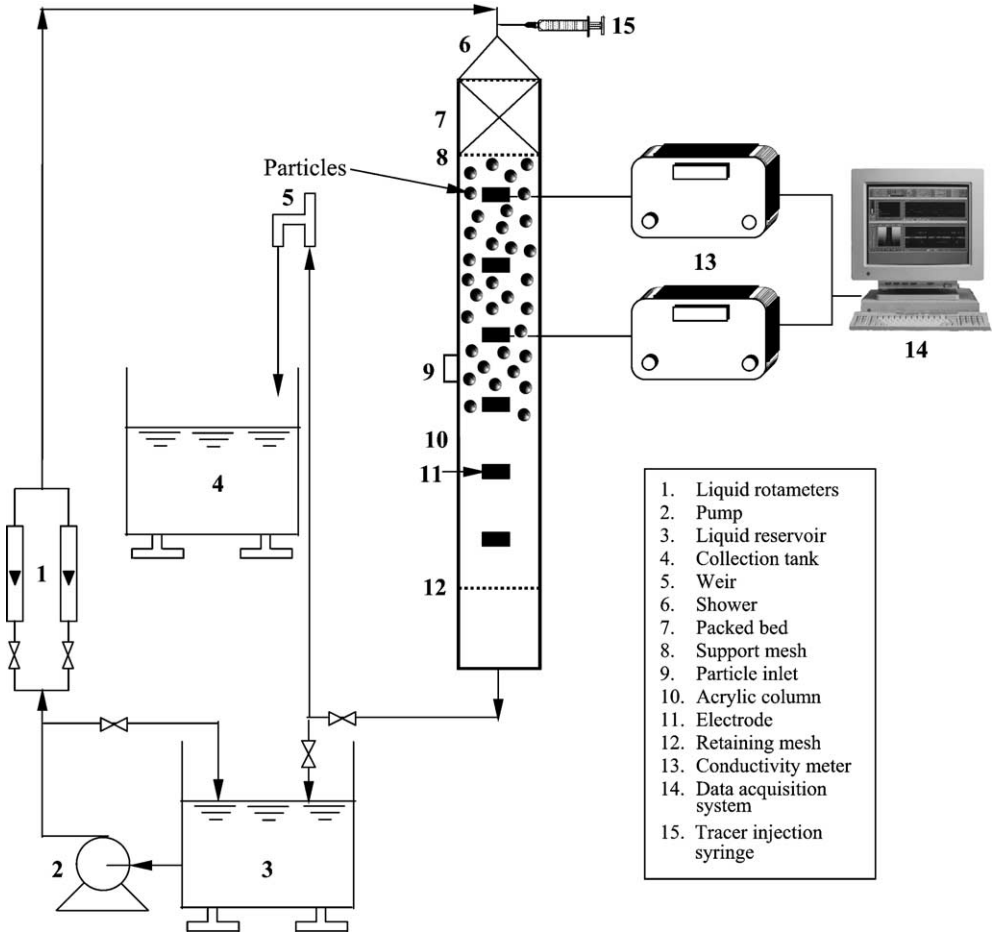

Fig. 1. Schematic diagram of experimental setup.

The convolution integral equation is given by

$$E_{\text{out}}(t) = \int_0^t f(\tau, Pe) E_{\text{in}}(t-\tau)\mathrm{d}\tau \quad (1)$$

where $E_{\text{out}}(t)$ is the exit age distribution measured at 2nd measuring point, $E_{\text{in}}(t)$ is the exit age distribution measured at 1st measuring point, $f(\tau,Pe)$ is the axial dispersion model impulse response function given by

$$f(\tau, Pe) = \frac{1}{2}\left(\frac{Pe}{\pi\theta^3}\right)^{1/2} \exp\left[-\frac{Pe}{4}\frac{(\theta-1)^2}{\theta}\right] \quad (2)$$

where $\theta = t/\tau$ is the dimensionless residence time of the system. The optimal values of the parameters Pe and τ are obtained by least-square minimization of objective function (using the function 'leastsq' in MATLAB®):

$$J = \sum (E_{\text{out}} - E_{\text{out,prd}})^2 \quad (3)$$

where $E_{\text{out,prd}}$ is $E(t)$ predicted at 2nd measuring point (calculated from Eq. (1) using fast Fourier transform). Using Pe and τ obtained from the above procedure, the RTD of the system is obtained from the equation for the axial dispersion model with open–open boundary conditions given by [6]

$$E(\theta) = \frac{1}{2}\left(\frac{Pe}{\pi\theta}\right)^{1/2} \exp\left[-\frac{Pe}{4}\frac{(\theta-1)^2}{\theta}\right] \quad (4)$$

4. Results and discussion

The measured input and output $E(t)$ curves are shown in Fig. 2 along with the RTD of the system for a typical experiment. The RTD of the system is obtained by deconvoluting the input RTD from output RTD. It is generally observed from the experiments that the spread in RTD curve (increase in mixing) increases with increase in flow rate, static bed height and Archimedes number.

As mentioned in the previous section, the mean residence time, τ, has been fitted as a parameter (through deconvolution procedure) and the same is compared with the mean residence time, τ_{hyd}, calculated from the following equation with an RMS error of 7.5% (Fig. 3):

$$\tau_{\text{hyd}} = \frac{\Delta z}{u_l/\varepsilon} \quad (5)$$

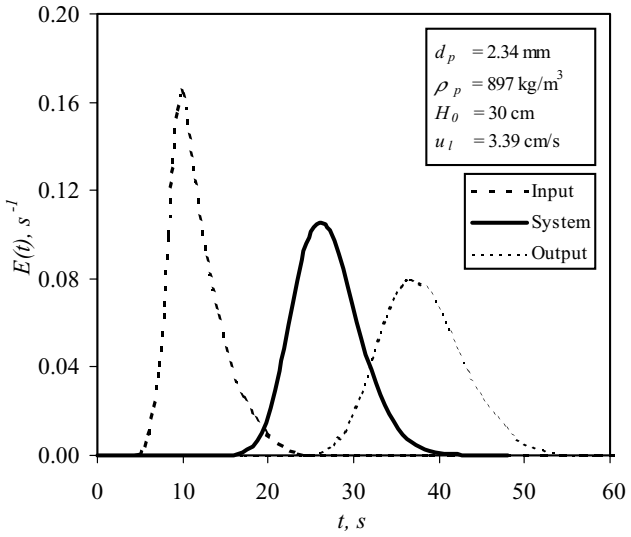

Fig. 2. Measured input and output RTD and system RTD (deconvoluted).

The voidage, ε, is measured through bed expansion by the conductivity method. The close agreement between residence time based on hydrodynamics and residence time based on RTD suggests that the dispersion is relatively low in the system for most of the experimental conditions.

4.1. Effect of parameters on liquid phase dispersion coefficient

The liquid phase axial dispersion coefficient is obtained from the optimal value of *Pe* found from the deconvolution procedure using the equation:

$$D_l = \frac{u_l \Delta z}{Pe\, \varepsilon} \tag{6}$$

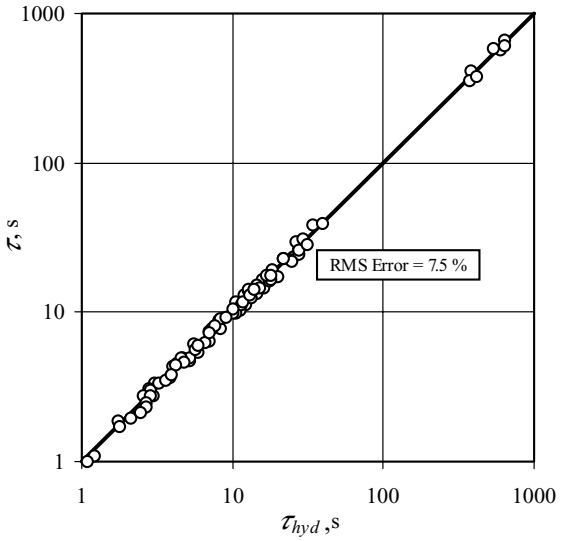

Fig. 3. Comparison of residence time from RTD and hydrodynamics.

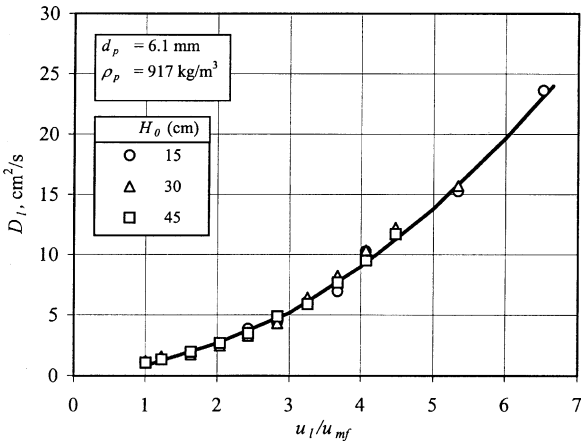

Fig. 4. Effect of liquid velocity on liquid phase dispersion coefficient.

where Δz is the distance between the two measuring points. The range of axial dispersion coefficients obtained in the present study are in the same range (D_l = 0.1–100 cm^2/s) reported in the literature for classical L-S fluidized beds [7–9].

4.1.1. Effect of liquid velocity

The variation in axial dispersion coefficient of liquid phase with normalized liquid velocity (normalized by u_{mf}) is shown in Fig. 4 with static bed height as parameter. It can be seen from this figure that the axial dispersion coefficient increases with increase in liquid velocity. With increase in liquid velocity, the movement of particles intensifies and thus the liquid in the bed is subjected to increasingly vigorous turbulence, resulting in the increase of mixing of the liquid phase. The increase in axial dispersion coefficient with liquid velocity is also observed by Chung and Wen [7], Krishnaswamy and Shemilt [8] and Tang and Fan [9] for classical L-S fluidized bed.

The liquid phase dispersion coefficient is reported to increase with increase in liquid velocity and reach a maximum at a velocity corresponding to a voltage around 0.7 and decrease with further increase in liquid velocity [8,10–12]. However, it is also observed by Chung and Wen [7] and Tang and Fan [9], a monotonic increase of dispersion coefficient with increase in liquid velocity even beyond voidage of 0.7.

The increase and decrease in the trend of dispersion coefficient with liquid velocity is usually observed for particle sizes of less than 1000 μm [8,10–12], whereas the monotonic increase in dispersion coefficient is reported for particle size of greater than 1000 μm [7,9]. The particles with size greater than 1000 μm used in the present study followed this reported monotonic increase in dispersion coefficient. This may be due to a sharp increase in the tube dispersion and a development of a specific particle circulation flow with increase in voidage beyond 0.7 [9].

In the present study, a particle of size 180 μm was also used in the experiments. Even these particles showed a

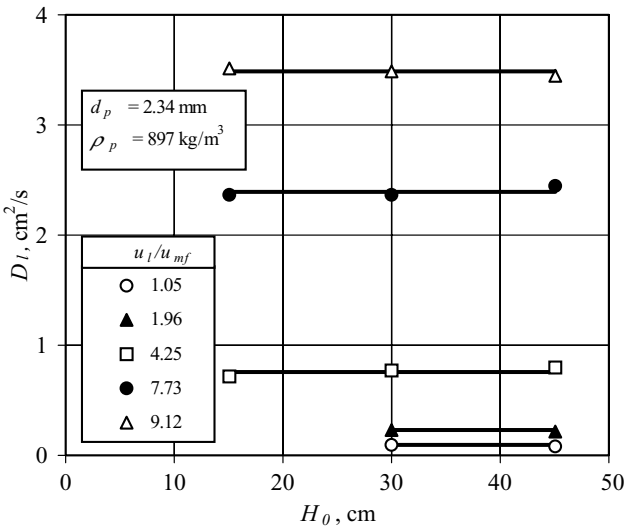

Fig. 5. Effect of static bed height on liquid phase dispersion coefficient.

monotonic increase in dispersion coefficient with liquid velocity which is against the reported trend in the literature for small particles in classical fluidized beds. In spite of repeated experiments, the same trend is observed. This particle has the lowest *Ar* of 17.6 in the present study, the next being 12947. To get better understanding of the variation of dispersion coefficient with liquid velocity in IFB, experiments with particles of *Ar* between 17.6 and 12947 may be necessary.

4.1.2. Effect of static bed height

The effect of static bed height on liquid phase axial dispersion coefficient is presented in Fig. 5 with normalized liquid velocity as parameter. It can be seen that the axial dispersion coefficient remains almost constant with increase in static bed height. This information is also given in Fig. 4. However, in Fig. 5 the effect is explicitly seen. The independency of axial dispersion coefficient with static bed height is also reported by Tang and Fan [9] in the case of classical L-S fluidized bed.

From the definition of Peclet number, D_l can be written as shown in Eq. (6). With increase in static bed height, Peclet number increases. At the same time, the expanded bed height also increases. Hence, the axial dispersion coefficient is almost constant within the experimental errors. In fact, in the formulation of axial dispersion model, D_l is constant along the length of the bed.

4.1.3. Effect of Archimedes number

Fig. 6 shows the effect of Archimedes number on liquid phase axial dispersion coefficient with normalized liquid velocity as parameter. It can be seen that the axial dispersion coefficient increases with increase in Archimedes number. With increase in Archimedes number, the minimum fluidization velocity increases and so the actual liquid velocity is more for a particle with a higher Archimedes number than for a particle with a lower Archimedes number even though the ratio u_l/u_{mf} may be same. Increased liquid velocity implies more axial dispersion coefficient as explained under the effect of liquid velocity. This explains the reason for the increasing trend of axial dispersion coefficient with Archimedes number which is also observed by Chung and Wen [7] and Tang and Fan [9] in classical L-S fluidized beds.

4.2. Correlation for liquid phase dispersion coefficient

Based on the experimental data from the present study, the following correlation is proposed to predict liquid phase

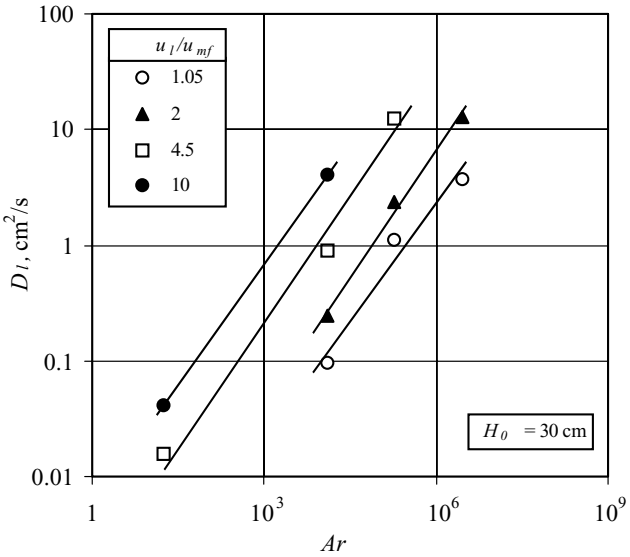

Fig. 6. Effect of Archimedes number on liquid phase dispersion coefficient.

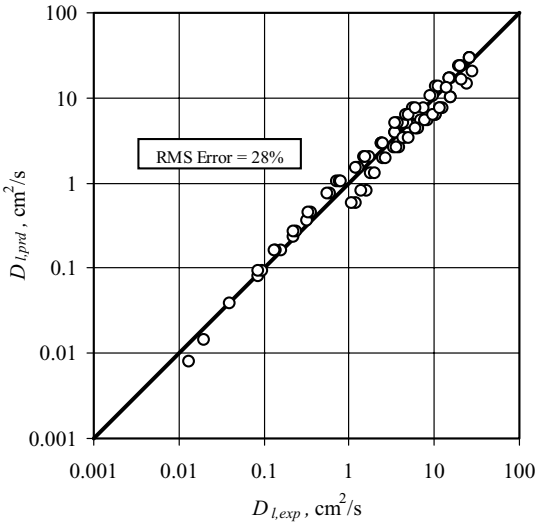

Fig. 7. Comparison of experimental and predicted liquid phase dispersion coefficient.

dispersion coefficient:

$$D_l(\mathrm{cm}^2/\mathrm{s}) = 1.48 \times 10^{-4} Ar^{0.66} \left(\frac{Re}{Re_{mf}}\right)^{1.73} \quad (7)$$

Here Re_{mf} is determined by Wen and Yu equation [13] as

$$Re_{mf} = \sqrt{(33.7)^2 + 0.0408\,Ar} - 33.7 \quad (8)$$

The validity of the Wen and Yu equation for determination of minimum fluidization velocity in 2-phase L-S IFB has been recently validated by the authors [14] using a vast amount of experimental data. Fig. 7 compares the experimental data of dispersion coefficient and values predicted from the above correlation (Eq. (7)) with an RMS error of 28%. The correlation is valid for $17.6 < Ar < 1.47 \times 10^7$ and $0.036 < Re < 1267$.

5. Conclusions

The mixing characteristics of the liquid phase in 2-phase L-S IFB has been studied for the first time in the literature. The liquid phase axial dispersion coefficient increases with increase in liquid velocity and Archimedes number and is independent of static bed height. An empirical correlation has been proposed for liquid phase axial dispersion coefficient in 2-phase IFB. To understand the variation in liquid phase dispersion coefficient with liquid velocity for particles having *Ar* between 17.6 and 12947, more studies are required.

Acknowledgements

The authors wish to express their gratitude to Envirospheres Pty Ltd., P.O. Box 497, Lindfield NSW 2070, Australia for their kind help of supplying 10 kg of microglass spheres (Espheres^{TM}).

References

[1] L.-S. Fan, Gas–Liquid–Solid Fluidization Engineering, Butterworths, Stoneham, 1989.
[2] L. Nikolov, D. Karamanev, Experimental study of the inverse fluidized bed biofilm reactor, Can. J. Chem. Eng. 65 (1987) 214–217.
[3] D.G. Calderon, P. Buffiere, R. Moletta, S. Elmaleh, Anaerobic digestion of wine distillery wastewater in down-flow fluidized bed, Wat. Res. 32 (1998) 3593–3600.
[4] C. de Boor, A Practical Guide to Splines, Springer-Verlag, New York, 1978.
[5] M.L. Michelsen, A least-squares method for residence time distribution analysis, Chem. Eng. Sci. 4 (1972) 171–179.
[6] O. Levenspiel, W.K. Smith, Notes on the diffusion-type model for the longitudinal mixing of fluids in flow, Chem. Eng. Sci. 6 (1957) 227–233.
[7] S.F. Chung, C.Y. Wen, Longitudinal dispersion of liquid flowing through fixed and fluidized beds, AIChE J. 14 (1968) 857–866.
[8] P.R. Krishnaswamy, L.W. Shemilt, Frequency response in liquid fluidized systems. Part I. Effect of particle density and size, Can. J. Chem. Eng. 51 (1973) 680–687.
[9] W.-T. Tang, L.-S. Fan, Hydrodynamics of a three-phase fluidized bed containing low-density particles, AIChE J. 35 (1989) 355–364.
[10] T.J. Hanratty, G. Latinen, R.H. Wilhelm, Turbulent diffusion in particulately fluidized beds of particles, AIChE J. 2 (1956) 372–380.
[11] E.J. Cairns, J.M. Prausnitz, Macroscopic mixing in fluidization, AIChE J. 6 (1960) 554–560.
[12] K.-I. Kikuchi, H. Konno, S. Kakutani, T. Sugawara, H. Ohashi, Axial dispersion of liquid in liquid fluidized beds in the low Reynolds number region, J. Chem. Eng. Jpn. 19 (1984) 362–367.
[13] C.Y. Wen, Y.H. Yu, Mechanics of fluidization, Chem. Eng. Prog. Symp. Ser. 66 (1966) 101–111.
[14] T. Renganathan, K. Krishnaiah, Prediction of minimum fluidization velocity in 2- and 3- phase inverse fluidized beds, Can. J. Chem. Eng. 81 (2003) 853–860.